Clinical Cancer Research

Genomic Signatures Predict the Immunogenicity of BRCA-Deficient Breast Cancer

Adam A. Kraya[1], Kara N. Maxwell[2], Bradley Wubbenhorst[1], Brandon M. Wenz[1], John Pluta[1], Andrew J. Rech[2], Liza M. Dorfman[1], Nicole Lunceford[3], Amanda Barrett[3], Nandita Mitra[4], Jennifer J.D. Morrissette[5], Michael Feldman[3,6], Anupma Nayak[3], Susan M. Domchek[2,6,7], Robert H. Vonderheide[2,6,7], and Katherine L. Nathanson[1,6,7]

Abstract

Purpose: Breast cancers with *BRCA1/2* alterations have a relatively high mutational load, suggesting that immune checkpoint blockade may be a potential treatment option. However, the degree of immune cell infiltration varies widely, and molecular features contributing to this variability remain unknown.

Experimental Design: We hypothesized that genomic signatures might predict immunogenicity in *BRCA1/2* breast cancers. Using The Cancer Genome Atlas (TCGA) genomic data, we compared breast cancers with (89) and without (770) either germline or somatic *BRCA1/2* alterations. We also studied 35 breast cancers with germline *BRCA1/2* mutations from Penn using WES and IHC.

Results: We found that homologous recombination deficiency (HRD) scores were negatively associated with expression-based immune indices [cytolytic index ($P = 0.04$), immune ESTIMATE ($P = 0.002$), type II IFN signaling ($P = 0.002$)] despite being associated with a higher mutational/neoantigen burden, in *BRCA1/2* mutant breast cancers. Further, absence of allele-specific loss of heterozygosity (LOH negative; $P = 0.01$) or subclonality ($P = 0.003$) of germline and somatic *BRCA1/2* mutations, respectively, predicted for heightened cytolytic activity. Gene set analysis found that multiple innate and adaptive immune pathways that converge on NF-κB may contribute to this heightened immunogenicity. IHC of Penn breast cancers demonstrated increased $CD45^+$ ($P = 0.039$) and $CD8^+$ infiltrates ($P = 0.037$) and increased PDL1 expression ($P = 0.012$) in HRD-low or LOH-negative cancers. Triple-negative cancers with low HRD had far greater $CD8^+$ T cells ($P = 0.0011$) and Perforin 1 expression ($P = 0.014$) compared with hormone receptor-positive HRD-high cancers.

Conclusions: HRD scores and hormone receptor subtype are predictive of immunogenicity in *BRCA1/2* breast cancers and may inform the design of optimal immune therapeutic strategies.

Introduction

Mutations in *BRCA1* and *BRCA2* are the most common causes of hereditary breast cancer. BRCA1 and BRCA2 play essential functions in maintaining genome integrity, primarily through their roles in homologous recombination (HR) and contribution to double-strand DNA break repair (1). Breast cancers associated with germline *BRCA1* and *BRCA2* mutations have higher sensitivity to DNA-damaging agents including platinum-based chemotherapy and inhibitors of poly(ADP-ribose) polymerase (PARP1), as HR is necessary for repair of DNA crosslinks (1). However, outcomes can vary widely across patients with germline *BRCA1* and *BRCA2* mutations receiving DNA-damaging agents, which in part may be due to the varying degree of HR deficiency (HRD) in these tumors. Secondary genetic alterations, particularly *BRCA1/2* reversion mutations, lead to acquired resistance to these therapies, necessitating the investigation of alternative treatment strategies (2, 3).

Tumors with somatic or germline defects in *BRCA1/2* are hypothesized to be more immunogenic than tumors without genetic defects in the HR pathway, making them potential candidates for immune checkpoint blockade (4–7). *BRCA1/2*

[1]Division of Translational Medicine and Human Genetics, Department of Medicine, Perelman School of Medicine at the University of Pennsylvania, Philadelphia, Pennsylvania. [2]Division of Hematology/Oncology, Department of Medicine, Perelman School of Medicine at the University of Pennsylvania, Philadelphia, Pennsylvania. [3]Division of Surgical Pathology, Pathology and Laboratory Medicine, Perelman School of Medicine at the University of Pennsylvania, Philadelphia Pennsylvania. [4]Department of Biostatistics, Epidemiology, and Informatics, University of Pennsylvania, Philadelphia, Pennsylvania. [5]Division of Precision and Computational Diagnostics, Pathology and Laboratory Medicine, Perelman School of Medicine at the University of Pennsylvania, Philadelphia, Pennsylvania. [6]Abramson Cancer Center, Perelman School of Medicine at the University of Pennsylvania, Philadelphia, Pennsylvania. [7]Basser Center for BRCA, Perelman School of Medicine at the University of Pennsylvania, Philadelphia, Pennsylvania.

Note: Supplementary data for this article are available at Clinical Cancer Research Online (http://clincancerres.aacrjournals.org/).

A.A. Kraya and K.N. Maxwell contributed equally to this article.

R.H. Vonderheide and K.L. Nathanson jointly supervised the work.

Corresponding Author: Katherine L. Nathanson, University of Pennsylvania, Philadelphia, PA 19104. Phone: 215-662-4740; E-mail: knathans@upenn.edu

Clin Cancer Res 2019;25:4363–74

doi: 10.1158/1078-0432.CCR-18-0468

Translational Relevance

Immune checkpoint blockade has been put forward as a potential treatment strategy in *BRCA1/2* mutant breast cancers due to their genomic instability. However, only ∼20% of advanced triple-negative breast cancers, the most common subtype of *BRCA1* mutation-associated breast cancers, benefit from single-agent PD1/PDL1 therapy. This heterogeneity in response is likely due to variability in intrinsic immune infiltration. Here, we demonstrate that levels of homologous recombination deficiency (HRD) are inversely associated with immunogenicity in primary *BRCA1/2* breast cancers, a phenotype further modulated by hormone receptor expression. As efforts in the clinic continue to advance combinations of immune checkpoint blockade, PARP1 inhibitors, and platinum chemotherapy for patients with *BRCA1/2* mutation-associated cancers, our findings may help direct optimal trial design and interpretation.

mutation-associated breast cancers have been found to be more genomically unstable than tumors without such genetic alterations (2), with increased numbers of nonsynonymous single-nucleotide variants (SNV) likely driving the heightened immunogenicity observed in these tumors (6, 7). BRCA1/2 deficiency also has been associated with an immune activation signature (6), and histopathologic analyses have found that the level of lymphocytic infiltrates is the strongest positive predictor for recurrence-free survival in *BRCA1/2* mutation-associated breast cancer cases (6). Breast cancers with a DNA damage response-deficient phenotype, characterized by a 44-gene expression signature reflecting defects in the Fanconi anemia (FA)/BRCA DNA repair pathway, have been shown to have higher $CD4^+$ and $CD8^+$ T-cell infiltrates, likely driven by the release of chemoattractive cytokines through STING/TBK1/IRF3 signaling (5).

However, there is a wide range in immunogenicity observed in *BRCA1/2* mutation-associated breast cancers, and the molecular underpinnings of that variability have not been delineated (4–8). Although *BRCA1/2*-deficient breast cancers are generally more immunogenic than sporadic cancers (8), a comprehensive histopathologic analysis of *BRCA1/2* mutation-associated breast cancers found that greater than 50% were characterized by "absent/mild" levels of tumor-associated lymphocytes (4). Immune metagene signatures that provide an RNA-based measure of immune cytotoxicity demonstrate that immune gene expression ranges widely among *BRCA1/2*-deficient breast cancers (6). Further, triple-negative breast cancers (TNBC), the most common tumor type associated with germline *BRCA1* mutations, have shown a clinical response rate to PD1 checkpoint blockade monotherapy of only 18.5% (9, 10), underscoring the heterogeneity of *BRCA*-deficient breast cancers with respect to immunogenicity. Mouse models of Brca1 deficiency have also demonstrated that efficacy of CTLA4 and PD1 therapy in breast cancer may be dependent on concomitant treatment with DNA-damaging agents (7). A pan-cancer analysis of The Cancer Genome Atlas (TCGA) data found that the levels of genomic copy number variations (CNV) inversely correlate with a cytotoxic immune signature and clinical benefit from immune checkpoint blockade (11). Given that *BRCA1/2* cancers are characterized by unique genomic scars driven by CNVs (2, 3), this finding raises the question of whether mutational burden or CNV level might predominate in driving immunogenicity in *BRCA1/2* mutation-associated cancers.

Herein, we aimed to determine the underlying molecular features of immunogenicity in 115 *BRCA1*- and *BRCA2*-deficient breast cancers using genomic data from TCGA, and genomic and histopathologic analyses in a validation cohort ($n = 35$) from the Hospital of the University of Pennsylvania. We further aimed to stratify *BRCA1/2* breast cancer immunogenicity based on these features and understand the molecular processes underlying the immunogenic and nonimmunogenic phenotypes.

Materials and Methods

Acquisition of Penn and TCGA sequencing datasets

Level 1 DNA sequencing data for breast tumors from TCGA were obtained by submitting a project request for approval by the National Center for Biotechnology Information Genotypes and Phenotypes Database (NCBI dbGaP) Data Access Request System Protocol #5309 "*BRCA1* and *BRCA2* mutations in breast and ovarian cancer." Breast cancers with controlled-access Level 1 whole exome sequencing (WES) binary alignment map (*.bam) files were identified in the Genomic Data Commons (GDC; https://gdc.cancer.gov; $n = 1{,}098$ breast tumors). After filtering samples without RNAseq data or that failed to pass our quality control pipeline (2), 859 breast tumor/normal *.bam files in total were subjected to downstream analysis. RNAseq v2 expression data and patient clinical data for breast invasive carcinoma (TCGA, provisional) were downloaded from cBioportal (http://www.cbioportal.org/). Tumors were categorized as receptor positive or as TNBC using primary data from the Santa Cruz Cancer Genetics Hub (Supplementary Table S1).

DNA sequencing data from a discovery study population ascertained from academic and community hospital sites within Penn Medicine were used for this analysis. Briefly, informed consent was obtained from each participant for use of their samples in genetic studies in an IRB-approved study. Patients with diagnosis of breast cancer and mutations identified though germline *BRCA1/2* sequencing in a Clinical Laboratory Improvement Amendments (CLIA)-approved laboratory were eligible. As previously described (2), formalin-fixed paraffin-embedded (FFPE) tumor blocks were macrodissected, sectioned, and stained with hematoxylin and eosin to ensure sections of over 70% invasive tumor. Tumors passing pathology quality control were dissolved in Deparaffinization Solution (Qiagen) and purified using Gentra PureGene Tissue Kit (Qiagen) following manufacturer's protocols. DNA libraries were subjected to WES using the Agilent All-Exon Kit v5, and matched tumor and normal sequencing data for 43 breast cancer patients (*BRCA1*, $n = 25$; *BRCA2*, $n = 18$) were used for HLA typing.

Analysis of Penn and TCGA WES data

All WES data from TCGA tumors and matched germline were aligned to the hg38 assembly of the human genome. All WES data from Penn tumors and matched germline were aligned to the hg19 assembly of the human genome. Alignment data underwent initial quality control filtering according to GATK best practices. All exonic germline and somatic SNVs, and germline *BRCA1* and *BRCA2* mutations were identified and annotated as previously described (2). Exonic variants were annotated as somatic, if they had an alternate allele depth in germline of less than five reads and

an alternate allele supported by greater than 10 reads in the tumor. Tumors were determined to be associated with germline *BRCA1* and *BRCA2* mutations if the germline allelic fraction (AF) >0.30 for the mutation, and the total depth was >30 in germline and tumor at the mutation locus. Only tumors with known pathogenic *BRCA1* or *BRCA2* mutations as per ENIGMA classification (43) were retained (Supplementary Tables S1 and S2). In total, we identified 35 breast tumors from the TCGA associated with germline *BRCA1* ($n = 18$) or *BRCA2* ($n = 17$) mutations with RNAseq data. We also studied 43 breast tumors with germline *BRCA1* ($n = 25$) or *BRCA2* ($n = 18$) mutations identified from Penn, 35 of which had available tumor for IHC staining (*BRCA1* = 23, *BRCA2* = 12).

Allele-specific LOH of the germline *BRCA1/2* mutation in the tumor was determined through a combination of Varscan2 (44), purity-adjusted allele frequency comparisons, and allele specific copy number calls as previously described (2). Briefly, estimates of tumor purity and ploidy were determined using Sequenza (45) for use in Varscan2 variant calling. Samples with a significant Varscan2 somatic *P*-value were assigned an allele-specific LOH-positive status and those with a significant Varscan2 germline *P*-value were assigned an allele-specific LOH-negative status. Sequenza was also used to call allele-specific copy number states in the genomic region containing the *BRCA1* or *BRCA2* mutation. The copy number of the genomic region surrounding the germline *BRCA1* or *BRCA2* mutation (CN) and the number of mutant alleles (m) were used to assign LOH states, including allele-specific LOH positive ($CN = 1$, $m = 1$; $CN = 2$, $m = 2$; or $CN > 2$, $m = 2$) and allele-specific LOH negative ($CN = 2$, $m = 1$; or $CN > 2$, $m = 1$; Supplementary Table S1).

Using our mutation calling pipeline (2), level 3 RNAseq *z*-scores, microarray *Z*-scores, and HK27/HK450 methylation β values from The Cancer Genomics Hub (https://gdc.cancer.gov/) for the tumor/normal pairs, we identified 54 additional breast tumors with somatic alterations in *BRCA1* or *BRCA2* that met the following criteria: (i) presence of a deleterious or likely deleterious single nucleotide or insertion/deletion variant using our previously described variant annotation pipeline (2); (ii) RNAseq *z*-score < −1.5 for *BRCA1* expression (with HK450m >0.5 or data not available); and (iii) *BRCA1* or *BRCA2* homozygous copy loss by Sequenza analysis (Supplementary Table S1). HR gene mutated breast cancers included those harboring: (i) deleterious or likely deleterious single nucleotide or insertion/deletion variants at other genes involved in HR (12) as defined in Supplementary Table S3; (ii) promoter methylation HK450m >0.25 with RNAseq←1.5 for *RAD51C*; (iii) *PTEN* homozygous copy loss or clonal mutation (12); and (iv) *EMSY* high copy gain (ref. 12; Supplementary Tables S1 and S3). Finally, tumors with no identifiable alteration in *BRCA1/2* or other HR-related genes were classified as HR wild-type tumors. HRD scores were determined using custom R-scripts (2) and Sequenza (45), which assigned counts of non-telomeric allelic imbalance (NtAI), large state transitions (LST), and genomic LOH (2, 3).

Determination of mutational burden, HLA types, and neoantigen load

All SNVs described in ref. 2 were used to calculate mutational burden. We defined mutational burden as the number of non-synonymous somatic mutations per megabase of genomic DNA. We determined HLA genotypes from germline TCGA and Penn WES files using OptiType (46) requiring a minimal read depth of 40 at the HLA loci; clinical HLA typing in a subset of non-TCGA samples ($n = 7$) showed complete concordance with OptiType calls (Supplementary Table S4). Neoantigen prediction was accomplished through NetMHCcons (47) called from the Immune Epitope Database Application Programming Interface (IEDB-API). All samples met the minimum read depth requirements and were retained for downstream analysis. Epitope lengths of 8, 9, and 10 were queried from FASTA files for each patient containing peptide sequences of length 15, 17, and 19, respectively. All neoantigens with a predicted IC_{50} <500 nmol/L and a rank score of less than 2% were retained for comparisons across tumor groups.

Transcriptomics analysis of TCGA tumors

Cytolytic index for each tumor was computed as the geometric mean of *PRF1* and *GZMA* expression from RNAseq v2 expression data downloaded from cBioportal (http://www.cbioportal.org/), as noted above. Inference of immune cell infiltration from TCGA RNA-Seq data was accomplished via the "estimate" R package (14). ESTIMATE gives a measure of immune cell infiltration by performing single-sample gene set enrichment analysis (ssGSEA) based on an inferred immune signature. The immune signature represents the intersection between two gene sets: a leukocyte methylation signature gene set and genes enriched for high expression in normal hematopoietic cells.

Gene Set Variation Analysis (GSVA) was implemented via the "gsva" Bioconductor package (48). All curated canonical pathways (C2) were downloaded from the Molecular Signatures Database (49) (http://software.broadinstitute.org/gsea/msigdb/genesets.jsp?collection=CP), and GSVA scores were determined for all breast tumors. Immune metagene gene sets for GSVA were obtained from Rooney and colleagues (13).

CD3, CD4, CD8, CD20, CD45, CD68, FoxP3, PRF1, and PDL1 IHC

Tissue microarrays for Penn breast *BRCA1/2* tumors were prepared as previously described (2). IHC was performed using mouse monoclonal antibodies for CD3 (Leica Biosystems, Catalog No. PA0553), CD8 (Dako, Catalog No. M7103), CD20 (Dako, Catalog No. M0755), CD45 (Dako, Catalog No. M0701), CD68 (Dako, Catalog No. M0814), FoxP3 (Biolegend, Catalog No. 320102), and PRF1 (Leica Biosystems, NCL-L-Perforin), and a rabbit monoclonal antibody for PDL1 (Cell Signaling Technology, 15161 BF). Scoring for IHC stains was performed in triplicate for each sample, and normalized counts of CD3, CD8, and PRF1-positive cells were determined by board-certified pathologists (A. Barrett, M. Feldman, and A. Nayak). PDL1 stain intensity was graded on a four-point scale (0–3) by board-certified pathologists (A. Barrett and M. Feldman), with 0 = *no staining*, 1 = *weak or partial staining*, 2 = *moderate staining*, 3 = *strong staining*. PDL1 H-scores were computed for statistical comparisons across tumor subsets.

Masson's trichrome staining

Masson's trichrome staining was accomplished with a Staining Kit from Polysciences, Inc. (Catalog No. 25088). Tissue microarray sections were fixed in Bouin's solution at 60°C and washed. Fixed sections were stained with the following reagents: Weigert's Iron Hematoxylin, Beibrich Scarlet-Acid Fuchsin, phosphotungstic acid, and Aniline Blue. At the conclusion of the staining protocol, all sections were rinsed with 1% acetic acid, dehydrated, and mounted for microscopy. Staining intensity was quantified by

board-certified pathologists (A. Nayak and M. Feldman) by grading on a four-point scale (0–3) of density and thickness for each trichrome stain (blue: collagen; red: myofibroblasts; black: nuclei). Density and thickness metrics were multiplied for each sample for statistical analysis.

Statistical analysis

Median HRD-total scores were determined for *BRCA1/2* (media, $n = 50.65$), HR mutant (media, $n = 12.08$), and HR wild-type (median $= -4.58$) tumors and used as the basis for dichotomization for each group of tumors. *P*-values for correlation between gene expression and sample traits (HRD and allele-specific LOH status) were calculated via the two-sided Student *t* test on log-normalized expression data. Normalized enrichment scores from GSVA were computed by setting "max.diff" to "TRUE," which provides a unimodal and approximately Gaussian distribution of enrichment scores (48). All linear statistical tests with GSVA scores were implemented via the "limma" package in R (50). T-statistics were adjusted using an empirical Bayesian model, and *P*-values were adjusted using the Benjamini–Hochberg method.

Cumulative hazard was compared using a Cox proportional hazards model to determine the effects of HRD level in breast patients, adjusting for stage, mutational burden, node positivity, and estrogen receptor expression status. Hazard curves were constructed in R using the "survival" (https://CRAN.R-project.org/package=survival) package

Data availability

The WES data that supports this study have been deposited in the National Center for Biotechnology Information (NCBI)'s Sequence Read Archive (SRA, https://www.ncbi.nlm.nih.gov/sra) with BioProject ID PRJNA38804 and can be accessed at: http://www.ncbi.nlm.nih.gov/bioproject/388048. The TCGA data are available from the National Cancer Institute's Genome Data Commons (https://gdc.cancer.gov/). The remaining data are available within the article and its Supplementary Information files or available from the authors upon request.

Results

Association of HRD with mutational and neoantigen burden in TCGA breast cancers

We investigated immunogenicity in breast cancers from TCGA (Supplementary Fig. S1A), including those with germline or somatic alterations in *BRCA1* or *BRCA2*, in non-*BRCA1/2* genes involved in HR (HR mutant tumors; ref. 12), and in those without alterations in genes involved in HR (HR wild-type tumors; Supplementary Tables S1 and S3). Mutational burden was higher in breast cancers associated with mutations in *BRCA1/2* ($P = 0.006$) and HR genes ($P = 8E{-}06$; Fig. 1A) than HR wild type. *BRCA1* expression was significantly lower in cancers with germline or somatic *BRCA1* alterations ($P = 0.026$), and expression of *BRCA2* was lower in cancers with *BRCA2* germline or somatic alterations with borderline significance ($P = 0.087$; Supplementary Fig. S1B). We determined neoantigen load (Supplementary Fig. S1C), which was also higher among *BRCA1/2* mutation-associated ($P = 0.014$) and HR gene mutation-associated ($P = 0.015$) breast cancers than among WT tumors (Fig. 1B). Notably, neoantigen load was not significantly different when comparing *BRCA1* versus *BRCA2* mutant tumors, tumors with germline versus somatic mutations in *BRCA1* or *BRCA2*, or nascent versus whole genome amplified (WGA) DNA (Supplementary Fig. S1D–S1F); thus, all were combined into a single *BRCA1/2* tumor group for further analyses.

We determined the HRD score for each tumor (2, 3), as described previously (2). We found that HRD score was higher among *BRCA1/2* mutation-associated versus HR gene mutation-associated ($P = 1.28E{-}09$) or HR gene wild-type breast cancers ($P = 3.03E{-}22$; Supplementary Fig. S1G). Dichotomizing tumors by median HRD score, we found that high HRD scores significantly correlated with increased neoantigen load amongst *BRCA1/2* ($P = 0.02$) and HR gene mutation-associated breast cancers ($P = 0.016$; Fig. 1C). Notably, HRD scores and estimated tumor ploidy also correlated with focal CNV levels and chromosome/arm CNV levels, respectively, as computed in a pan-TCGA cancer analysis (11) (Supplementary Fig. S2A). *BRCA1/2* cancers with higher HRD tended to exhibit a greater degree of aneuploidy (HRD high mean ploidy = 3.6, HRD low mean ploidy = 3.1, $P = 0.047$) than HRD-low cancers. These data show that deficiency in the HR pathway is correlated with genomic instability and an increase in predicted neoantigens.

HRD and immunogenicity in TCGA breast cancers

To infer immunogenicity in *BRCA1/2* mutation-associated breast cancers, we computed cytolytic index (13) as a measure of $CD8^+$ T-cell cytotoxicity and immune ESTIMATE scores (14) as a measure of lymphocyte infiltration. Neither immune measure differed between breast cancers with mutations in *BRCA1* and *BRCA2* nor germline versus somatic alterations (Supplementary Fig. S2B and S2C); hence, all tumors were combined for further analysis. We then investigated the association of these immune metrics with HRD level. Cytolytic index was higher in *BRCA1/2* mutation-associated ($P = 0.0016$) and HR gene mutation-associated ($P = 0.0019$) than HR wild type breast cancers (Fig. 1D), consistent with prior reports that HR pathway deficiency leads to increased immunogenicity (4–7). Unexpectedly, when *BRCA1/2* mutant breast cancers were dichotomized by median HRD score, higher HRD scores were associated with lower cytolytic index ($P = 0.043$) and immune ESTIMATE score ($P = 0.002$), despite correlating with a higher predicted neoantigen load (Fig. 1E and F). The magnitude of both immune metrics was independent of tumor stage (Supplementary Fig. S2D). Importantly, HRD-high BRCA1/2 cancers more closely resembled HR wild-type cancers (cytolytic index: *BRCA1/2* HRD high = 132.7, HR wild type = 118.5, $P = 0.56$; immune ESTIMATE score: *BRCA1/2* HRD high = −2.7, HR wild type = 191.1, $P = 0.12$). We also interrogated immune metagenes (13) by GSVA and found lower enrichment of the type II IFN metagene ($P = 0.002$; Fig. 1G) among HRD-high *BRCA1/2* mutation-associated breast cancers, suggesting lower immune effector activity in this tumor subset. HRD-low breast cancers were also associated with a significantly lower death hazard ratio from Cox proportional hazards analysis ($P = 0.03$; Supplementary Fig. S2E).

To gain further insight into factors that may contribute to lower immunogenicity in HRD-high *BRCA1/2* mutated breast cancers, we compared all curated, canonical pathways (MSigDb) by GSVA (Supplementary Fig. S2F; Supplementary Table S5). Multiple pathways including Notch, tumor necrosis factor (TNF), and MAPK signaling linked to NF-κB, a key transcription factor involved in CD28-mediated T-cell activation and the expression of chemoattractive T-cell cytokines (15, 16), and were elevated

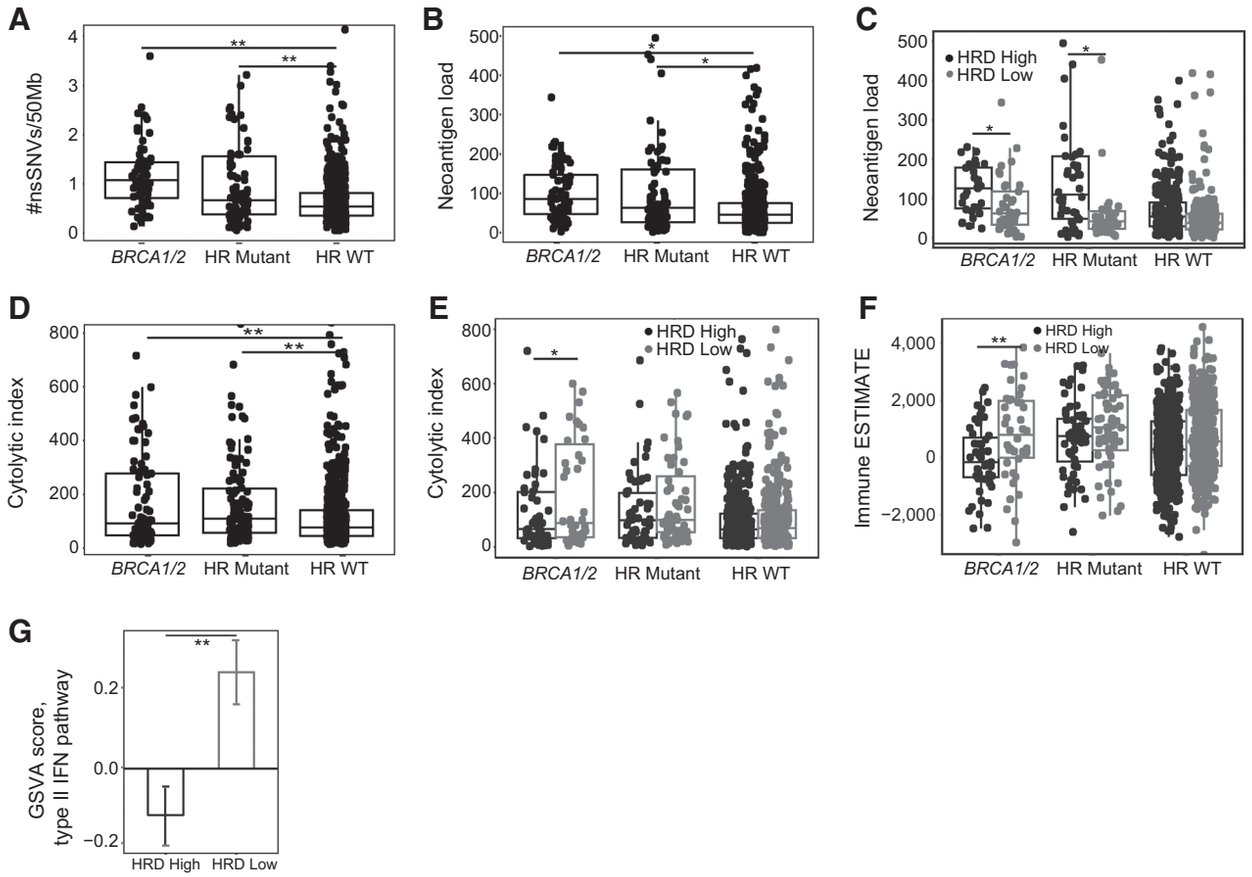

Figure 1.

Deficiency in the HR pathway confers increased mutational and neoantigen load but decreased immunogenicity in *BRCA1/2* mutation-associated breast cancer. In TCGA, (**A**) number of exonic nonsynonymous SNVs (nsSNV) per 50 megabases (Mb) in *BRCA1/2* mutation-associated ($n = 71$), HR mutant ($n = 91$), and HR wild-type ($n = 485$) breast tumors. **B,** Neoantigen load by HR mutation status. **C,** Neoantigen load by HR mutation status dichotomized by median HRD score. **D,** Cytolytic index across *BRCA1/2* mutation-associated ($n = 89$), HR mutant ($n = 118$), and HR wild-type ($n = 652$) tumors. **E,** Cytolytic index by median HRD level and *BRCA1/2* mutation status. **F,** Immune ESTIMATE score by median HRD level and BRCA1/2 mutation status. **G**, GSVA comparison of type II IFN signaling metagene by median HRD level in *BRCA1/2* mutation-associated tumors. Error bars, SE, *, $P < 0.05$, **, $P < 0.01$, Student *t* test. WT, wild type.

across HRD-low relative to HRD-high tumors (Supplementary Table S5). Type I IFN signaling, known to induce NF-κB activation and elicit antitumor immune responses in lymphocytes (17), was upregulated in HRD-low tumors ($P = 1.44E{-}14$). Pathways related to MAP-kinase-induced NF-κB activation from toll-like receptors ($P = 8.89E{-}04$, $P = 1.22E{-}03$, $P = 1.25E{-}03$), the pattern recognition receptors of innate immunity that play an important role in facilitating antigen-driven immune responses (18), were elevated in HRD-low tumors, likely mediated by altered IKK signaling observed in this subset ($P = 0.013$; ref. 18; Supplementary Table S5). Notch1 and Notch4 signaling, known to enhance $CD4^+$ and $CD8^+$ effector activity (19), also was elevated in HRD-low tumors ($P = 7.98E{-}3$, $P = 0.05$, respectively), both of which are capable of activating NF-κB canonical signaling (19). Elevated TGFβ signaling, observed in HRD-low tumors ($P = 0.045$), can induce NF-κB via TAK1 (20). Further, the TNF pathway can activate NF-κB specifically through the actions of TNFR1 and TNFR2 (21), both higher in HRD-low tumors ($P = 0.011$, $P = 0.016$), and promote antitumor immune responses by amplifying T-cell receptor (TCR)-induced signals. NF-κB activity can regulate the transcription of defensins and β-defensins, small cationic peptides involved in tumor suppression as well as in T-cell chemotaxis (22), and defensin-related pathways were found at far higher levels in HRD-low tumors ($P = 2.6E{-}36$, $P = 7.5E{-}34$). As STING (*TMEM173*) protein has been implicated in driving immunogenicity in DNA damage response-deficient (DDRD) breast cancers (5, 23) and acts through NF-κB (24), we also compared the expression of STING by HRD level and found that HRD-low tumors expressed higher levels of STING than HRD-high tumors ($P = 0.047$; Supplementary Fig. S2G). These data collectively suggest that low HRD BRCA1/2 breast cancers are associated with increased immunogenicity likely driven by NF-κB signaling.

Effects of complete loss of wild-type BRCA1/2 on breast cancer immunogenicity

Based on our prior work (2), we investigated whether allele-specific loss of heterozygosity (LOH) of the germline *BRCA1* or *BRCA2* mutation was predictive of immunogenicity in TCGA data. Allele-specific LOH was determined, as described

previously (2), by comparing purity-adjusted mutation allele frequencies and copy number states across matched tumor and normal samples (see "Materials and Methods"). Breast cancers with allele-specific LOH of the *BRCA1/2* germline mutation had significantly higher HRD score than tumors without allele-specific LOH (2). In the TCGA data set, we examined breast cancers associated with germline mutations in *BRCA2* only, including those with ($n = 10$, 59%) and without ($n = 7$, 41%) allele-specific LOH. We found that allele-specific LOH associated with germline mutations in *BRCA2* was associated with lower type II IFN signaling, cytolytic index, and immune ESTIMATE scores (Fig. 2A; $P = 0.01$, $P = 0.011$, $P = 0.039$, respectively). We observed a similar trend in breast cancers associated with germline *BRCA1* mutations, although only one breast cancer in the TCGA cohort lacked allele-specific LOH of the *BRCA1* mutation (Supplementary Fig. S3A). Given that the difference in immunogenicity dependent on heterozygous versus homozygous germline *BRCA1/2* mutations, we wanted to determine whether somatic *BRCA1/2* mutation clonality also was associated with differences in immunogenicity. We categorized all breast cancers with somatic mutations in *BRCA1/2* at a purity-adjusted allele frequency of less than 0.50 as subclonal ($n = 14$) to compare to cancers with either clonal mutations [corrected tumor allele frequency (CTAF) >0.50], promoter hypermethylation of *BRCA1*, and/or low

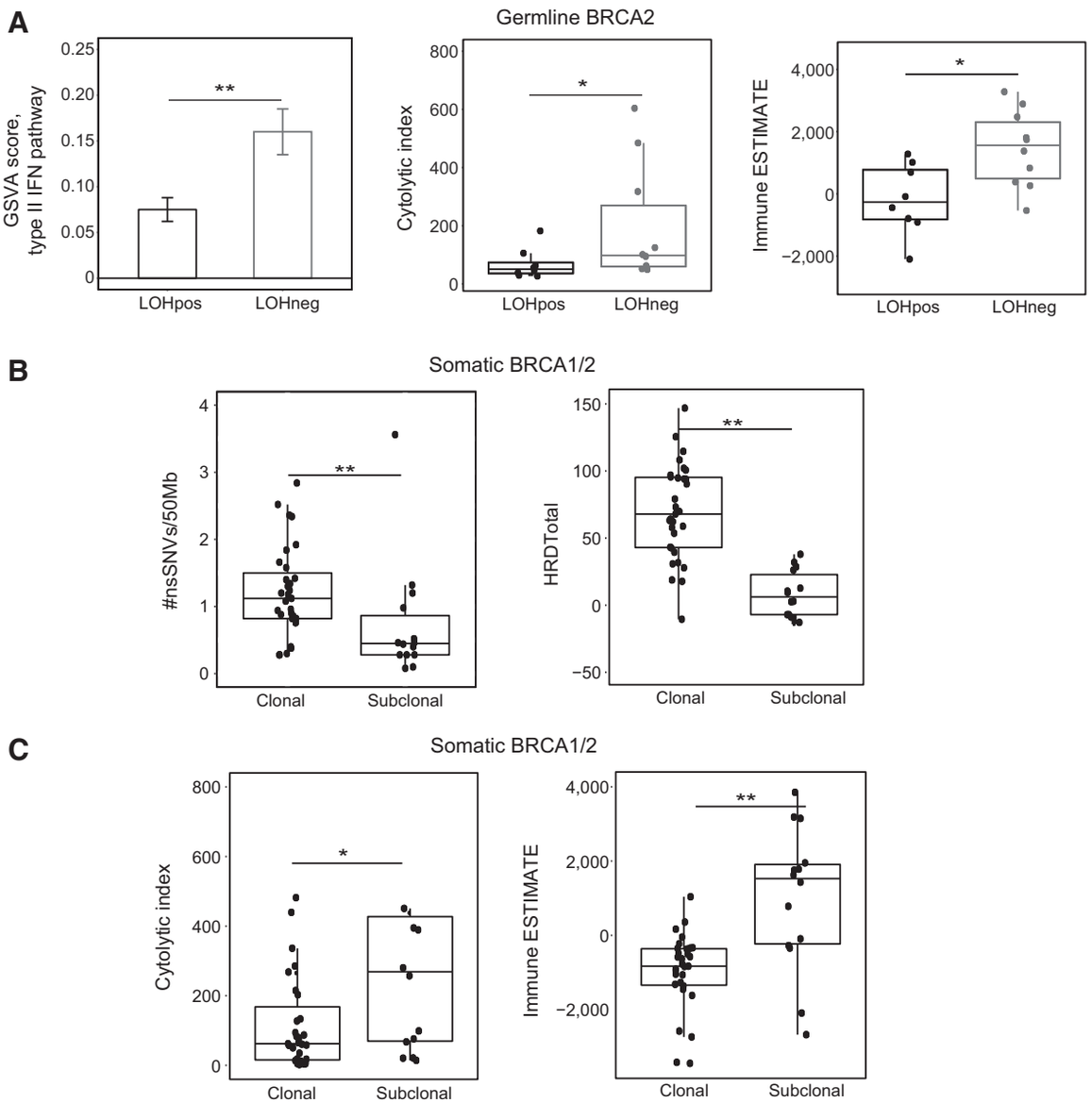

Figure 2.

Germline BRCA2 allele-specific LOH and clonal somatic *BRCA1/2* mutations correlate with lower immunogenicity in TCGA breast cancer. **A,** Type II IFN signaling, cytolytic index, and immune ESTIMATE score by *BRCA2* allele-specific LOH [LOH positive (LOHpos), $n = 7$; LOH negative (LOHneg), $n = 10$]. **B,** Mutational burden and HRD score by somatic *BRCA1/2* mutation clonality (subclonal, $n = 14$; clonal, $n = 33$). **C,** Cytolytic index and immune ESTIMATE score by somatic *BRCA1/2* mutation clonality (subclonal, $n = 14$; clonal, $n = 33$). Error bars, SE, *, $P < 0.05$; **, $P < 0.01$, Student *t* test.

expression (RNAseq *z*-score ←1.5 of *BRCA1* or *BRCA2* [referred to collectively as "clonal" *BRCA1/2* somatic mutation-associated cancers] ($n = 33$); Supplementary Table S1). We found that cancers with clonal *BRCA1/2* mutations had higher mutational burden ($P = 0.05$) and HRD scores ($P = 2.37E{-}07$; Fig. 2B), but lower cytolytic index ($P = 0.0033$) and immune ESTIMATE scores ($P = 4.98E{-}05$) than cancers with subclonal *BRCA1/2* mutations (Fig. 2C). When evaluating *BRCA1* cancers alone, we found that subclonal *BRCA1* alterations were associated with borderline significantly higher cytolytic index (subclonal: $n = 4$, mean cyt ind = 285.18; clonal: $n = 4$, mean cyt ind = 109.65; $P = 0.054$) and significantly higher immune ESTIMATE scores (subclonal, mean score = 1410.28; clonal, mean score = 71.81; $P = 0.022$). *BRCA2* cancers with subclonal alterations exhibited borderline significantly higher cytolytic index (subclonal: $n = 10$, mean cyt ind = 329.60; clonal: $n = 12$, mean cyt ind = 92.41; $P = 0.067$), and immune ESTIMATE scores (subclonal: mean score = 484.42; clonal: mean score = −227.48; $P = 0.079$). As STING can mediate inflammation through NF-κB and IRF7 (24), both of which were elevated in cancers with lower HRD, we then evaluated STING expression as a function of partial or complete loss of *BRCA1/2* function. We found that tumors with either *BRCA1/2* LOH or clonal somatic *BRCA1/2* alterations had lower STING expression than tumors negative for BRCA1/2 LOH or those with subclonal *BRCA1*/2 somatic mutations ($P = 0.04$ and $P = 2.1E{-}04$; Supplementary Fig. S3B). Collectively, these data suggest that the disparity in immunogenicity as a function of HRD in breast cancers is driven by full loss of *BRCA1* or *BRCA2* function, either by allele-specific LOH of a germline mutation or clonality of a somatic mutation.

Immune infiltrates and T-cell effector activity in Penn *BRCA1*/2 breast cancers

We performed IHC in breast cancers ascertained from Penn Medicine patients with confirmed germline *BRCA1* ($n = 23$) or *BRCA2* mutations ($n = 12$; Supplementary Fig. S3C; Supplementary Tables S1 and S2). We stained for multiple immune cell markers spanning adaptive and innate immune cell function including CD3, CD8, FOXP3, CD20, CD45, and CD68 in tissue microarray sections of *BRCA1/2* breast cancers. T cells (CD3, CD8, FOXP3), B cells (CD20), and cells of the myeloid lineage (CD68) were all detectable in our breast cancer set. Intratumoral, stromal, and total $CD8^+$ ($P = 0.0018$, 0.041, and 0.037, respectively) T cells were lower in *BRCA1/2* breast cancers with elevated levels of HRD (Fig. 3A and B), consistent with our results from our analysis of TCGA dataset, whereas no differences were observed in other immune markers (Supplementary Fig. S3D). Differences in $CD45^+$ T cells in association with HRD level were more strongly associated with *BRCA1* mutation-associated cancers (intratumoral, stromal, and total; $P = 0.032$, 0.043, and 0.039, respectively; Supplementary Fig. S3E and S3F). We investigated the effects of allele-specific LOH associated with germline mutations in *BRCA1* (LOH positive, $n = 18$, 78%; LOH negative, $n = 5$) and *BRCA2* (LOH positive, $n = 5$, 42%; LOH negative, $n = 7$) cancers. No significant differences were observed across $CD3^+$, $FOXP3^+$, and $CD68^+$ cells when analyzing germline *BRCA1/2* cancers collectively by allele-specific LOH status (Supplementary Fig. S3G). However, we found those that were *BRCA1/2* LOH positive had a lower number of $CD8^+$ T cells (intratumoral $P = 0.13$, stromal $P = 0.035$, and total $P = 0.015$), $CD20^+$ B cells (intratumoral $P = 0.043$, stromal $P = 0.223$, and total $P = 0.189$), and $CD45^+$ T cells (intratumoral $P = 0.002$, stromal $P = 0.041$, and total $P = 0.037$; Fig. 3C and D). Again, these changes were more strongly associated with *BRCA1* mutation-associated tumors; $CD8^+$ (intratumoral $P = 7.03e{-}5$, stromal $P = 0.0014$, and total $P = 0.00016$), $CD45^+$ (intratumoral $P = 0.00043$, stromal $P = 0.00014$, total $P = 8.0e{-}4$), and $CD20^+$ (intratumoral $P = 0.0345$, stromal $P = 0.0038$, and total $P = 0.0016$) cells were all found at lower levels in *BRCA1* allele-specific LOH-positive cancers (Supplementary Fig. S3H). Further, *BRCA1* allele-specific LOH-positive cancers specifically exhibited lower levels of $CD3^+$ (intratumoral $P = 0.016$, stromal $P = 0.0092$, total $P = 0.0067$) and $CD68^+$ (intratumoral $P = 0.019$, stromal $P = 0.106$, total $P = 0.140$) cells (Supplementary Fig. S3H). Differences for all cell types in *BRCA2* cancers were nonsignificant (Supplementary Fig. S3I). We stained for the programmed cell death protein ligand 1 (PDL1), a component of the dominant PD1–PDL1 immune checkpoint pathway induced by tumors to counter-regulate immune attack (25). We found lower levels of macrophage membrane ($P = 0.048$) and macrophage + tumor PDL1 ($P = 0.012$) in cancers with allele-specific LOH relative to cancers without allele-specific LOH (Fig. 3E and F), indicating lower tumor inflammation (25). These changes were driven by *BRCA1* cancers, whereby allele-specific LOH-positive cancers had lower macrophage membrane ($P = 0.019$) and total (tumor + macrophage, $P = 7.4e{-}4$) PDL1 relative to LOH-negative cancers (Supplementary Fig. S3J). *BRCA2* cancers trended in the same direction but failed to reach significance (Supplementary Fig. S3K).

Given that both TGFβ and NF-κB signaling were differentially regulated across HRD-high versus HRD-low tumors in TCGA cohort and given their known roles in remodeling the tumor microenvironment (Supplementary Table S5; refs. 26, 27), we investigated extracellular matrix composition by Masson's Trichrome staining in the Penn cohort (28). We found lower red myofibroblast staining in HRD-high versus HRD-low tumors ($P = 0.0071$; Fig. 3G and H).

Hormone receptor expression and HRD jointly stratify BRCA1/2 breast cancer immunogenicity

We analyzed the association between hormone receptor expression and immunogenicity in the background of *BRCA1/2* alterations, as TNBCs have been found to be generally more immunogenic than hormone receptor positive (Rec+) cancers (tumor types in Supplementary Table S1; ref. 6). Although there were no significant differences in cytolytic index and immune ESTIMATE within each hormone receptor subgroup based on *BRCA1* or *BRCA2* mutation status (Supplementary Fig. S4A), TNBCs had higher cytolytic index overall ($P = 0.025$; Fig. 4A) despite a similar mutational burden (Supplementary Fig. S4B). An expression level comparison of immunomodulatory genes across TNBCs and Rec+ *BRCA1/2* mutant breast cancers found that TNBCs had higher expression of most immune markers than Rec+ tumors, suggesting a more inflamed microenvironment (Fig. 4B; ref. 25). Inflamed tumors often express counter-regulatory checkpoint proteins such as PDL1 to evade immune attack (25). In Penn *BRCA1/2* germline mutation-associated breast cancers, membrane PDL1 was higher in TNBCs when summing with tumor and macrophage membrane PDL1 ($P = 0.035$; Fig. 4C).

We sought to investigate a potential interaction effect between HRD and hormone receptor statuses, performing a stratified

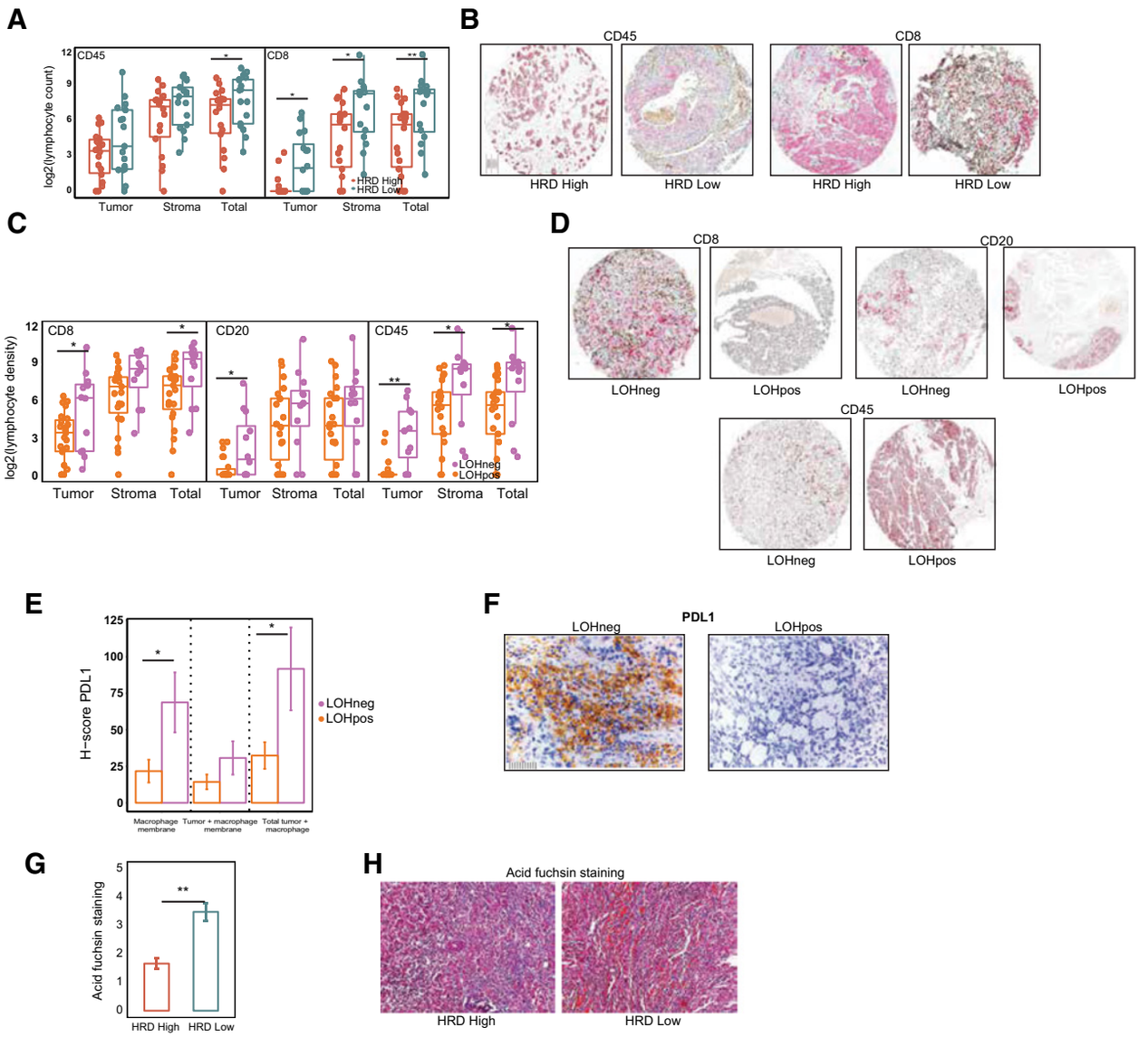

Figure 3.

Germline *BRCA1/2* allele-specific LOH and high HRD predict for lower tumor inflammation. In Penn *BRCA1/2* tumors, (**A**) levels of $CD45^+$ and $CD8^+$ immune cells by HRD level (high, $n = 17$; low, $n = 18$). **B,** Representative CD45 and CD8 IHC images by HRD status, 10×, scale bar represents 0.1 mm at 0.01 mm increments. **C,** Levels of $CD8^+$, $CD20^+$, and $CD45^+$ immune cells by LOH status (LOH positive, $n = 23$; LOH negative, $n = 12$). **D,** Representative $CD8^+$, $CD20^+$, and $CD45^+$ IHC images by LOH status, 40×, scale bar represents 0.1 mm at 0.01 mm increments. **E,** PDL1 H-score by germline *BRCA1/2* LOH status (LOH positive, $n = 23$; LOH negative, $n = 12$). **F,** Representative PDL1 IHC images, 20×, scale bar represents 0.1 mm at 0.01 mm increments. **G,** Masson's Trichrome (acid fuchsin) score by HRD level (high, $n = 14$; low, $n = 12$). **H,** Representative Masson's Trichrome-stained sections highlighting red myofibroblasts, 20×. *, $P < 0.05$; **, $P < 0.01$, Student *t* test. Error bars, SE. LOHneg, LOH negative; LOHpos, LOH positive.

comparison in *BRCA1/2* TCGA tumors. Comparing cytolytic index and immune ESTIMATE in TCGA, we found the greatest difference between TNBC HRD-low ($n = 10$) and Rec+ HRD-high *BRCA1/2* breast cancers ($n = 22$; $P = 0.0013$; Fig. 4D and E). Similarly, when partitioning by *BRCA1/2* allele-specific LOH status and hormone receptor expression, we found that TNBC, LOH-negative cancers had the highest cytolytic index ($n = 2$, mean cytolytic index = 303.1) at a borderline significantly higher level than Rec+, LOH-positive cancers ($n = 8$, mean cytolytic index = 97.7, $P = 0.052$), and Rec+, LOH-negative and TNBC, LOH positive had middling levels of cytolytic index (mean cytolytic index = 143.6 and 156.4, respectively). We confirmed these observations in Penn *BRCA1/2* germline mutation-associated breast cancers; LOH-positive cancers had significantly higher HRD score than LOH-negative cancers (Supplementary Fig. S4C; $P = 6.65e{-}6$). TNBC, LOH-negative ($n = 4$) cancers had the highest CD8 infiltrate when compared to TNBC, LOH-positive ($n = 14$; intratumoral $P = 9.22e{-}5$, stromal $P = 0.0063$, total $P = 0.0023$) and Rec+, LOH-positive ($n = 8$; intratumoral $P = 0.00051$, stromal $P = 0.0016$, total $P = 0.0011$) cancers, but

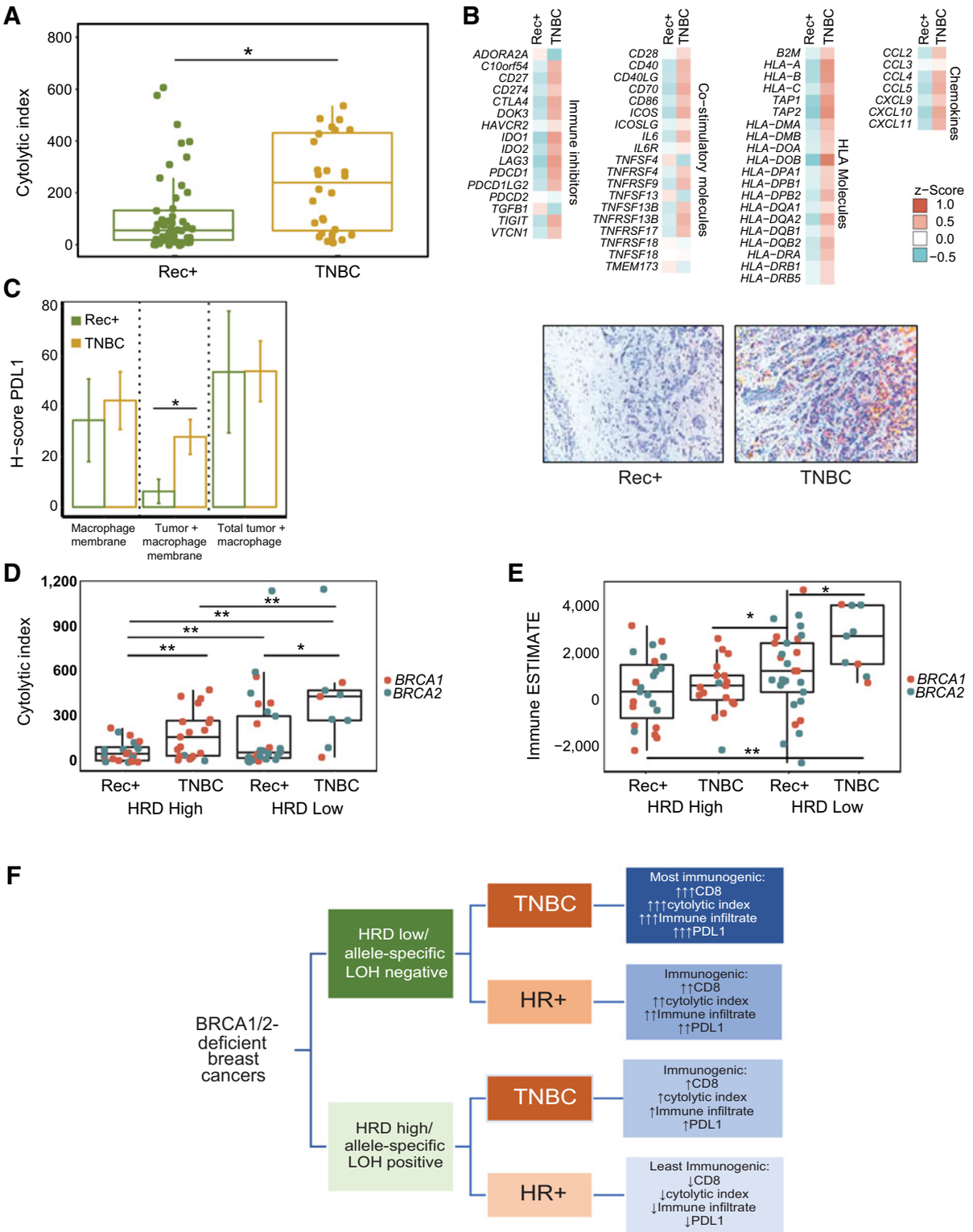

Figure 4.

Triple negativity and low HRD scores are features of immunogenic *BRCA1/2* breast tumors. **A,** In TCGA tumors, cytolytic index by receptor status (TNBC, $n = 30$; Rec+, $n = 53$). **B,** In TCGA tumors, immune-related gene expression by receptor status (TNBC, $n = 30$; Rec+, $n = 53$). **C,** In Penn tumors, PDL1 H-score by receptor status (TNBC, $n = 18$; Rec+, $n = 15$) and representative PDL1 IHC images, 20×. In TCGA tumors, interaction effect of receptor status and HRD level on cytolytic index (**D**) and immune ESTIMATE score (**E**; HRD high Rec+, $n = 22$; HRD low Rec+, $n = 31$; HRD high TNBC, $n = 20$; HRD low TNBC, $n = 10$). **F,** Model of immunogenicity illustrating the relative impact of receptor status, HRD, and allele-specific LOH of germline mutations in *BRCA1* and *BRCA2*. *, $P < 0.05$, **, $P < 0.01$, Student *t* test.

nonsignificantly higher than Rec+, LOH-negative ($n = 8$; intratumoral $P = 0.13$, stromal $P = 0.088$, total $P = 0.13$) cancers (Supplementary Fig. S4D). The same observations were found when comparing TNBC, LOH-negative to LOH-positive $CD3^+$ and $CD45^+$ infiltrates (CD3: intratumoral $P = 0.00024$, stromal $P = 0.038$, total $P = 0.0012$; CD45: intratumoral $P = 0.022$, stromal $P = 0.0022$, total $P = 0.0020$), Rec+, LOH-positive (CD3: intratumoral $P = 0.00073$, stromal $P = 0.014$, total $P = 0.0068$; CD45: intratumoral $P = 0.025$, stromal $P = 0.011$, total $P = 0.010$), and Rec+, LOH-negative (CD3: intratumoral $P = 0.068$, stromal $P = 0.069$, total $P = 0.066$; CD45: intratumoral $P = 0.021$, stromal $P = 0.041$, total $P = 0.044$) cancers (Supplementary Fig. S4E and S4F). Further, the number of PRF1-positive cells in the tumor microenvironment was highest in TNBC, LOH-negative cancers relative to TNBC, LOH-positive ($P = 0.024$), Rec+, LOH-positive ($P = 0.014$), and Rec+, LOH-negative ($P = 0.021$) cancers (Supplementary Fig. S4G). TNBC, LOH-negative membrane also had the highest levels of membrane and total PDL1 when compared with TNBC, LOH-positive (macrophage membrane $P = 0.015$, tumor+macrophage membrane $P = 0.039$, total $P = 0.034$) and Rec+, LOH-positive cancers (macrophage membrane $P = 0.012$, tumor+macrophage membrane $P = 0.028$, total $P = 0.013$), but not Rec+, LOH-negative cancers (macrophage membrane $P = 0.28$, tumor+macrophage membrane $P = 0.055$, total $P = 0.814$; Supplementary Fig. S4H).

Comparing all differentially regulated canonical pathways between these two groups in the TCGA (Supplementary Fig. S4I; Supplementary Table S6), we found that pathways related to TCR, chemokine, and PD1 signaling were the most positively upregulated in TNBC HRD-low tumors ($P < 0.005$). Collectively, these data suggest that HRD and hormone receptor expression independently stratify immunogenicity and, when considered jointly, can more precisely categorize the immune properties of *BRCA1/2* breast cancers.

Discussion

We have delineated the molecular properties of immunogenicity in breast cancers associated with *BRCA1/2* alterations (Fig. 4F); our observations have potential implications for treatment of these cancers with checkpoint blockade. *BRCA1/2*-mutation associated breast cancers exhibited slightly higher mutational load and predicted neo-epitopes compared with wild type tumors—features that were most prominent among the HRD-high subset; however, our findings now reveal that it is the HRD-low subset of breast cancers in this cohort that are the most highly immunogenic with the strongest evidence of CD8-driven T-cell responses. Thus, *BRCA1/2*-related breast cancers represent another example in which mutational burden and T-cell responses are not linked (29, 30); rather, tumor intrinsic features (31, 32) that regulate immune response and suppression are increasingly appreciated as driving forces. Further, our findings are consistent with a pan-cancer analysis which found that aneuploidy and a higher prevalence of large somatic copy number alterations, a feature of HRD, were associated with lower immune cytotoxicity, possibly due to these genomic events imparting dysfunction in cellular machinery involved in the recruitment of immune cells (11).

Immunogenicity in *BRCA1/2* breast cancers as a function of HRD may be related to multiple pathways that contribute to dendritic and T-cell function (Notch, TNF, and TLR signaling) that converge on NF-κB (21), a key proinflammatory transcription factor known to influence the transcription of genes involved in survival, inflammation, and lymphocyte activation (15) and shown to promote immune surveillance by augmenting the antitumor responses of T cells (16). As NF-κB signaling is influenced by DNA damage and *BRCA1/2* mutation status (33–36), our data collectively indicate that both tumor cell intrinsic (*BRCA1/2* and HRD) and extrinsic signals (TNF and TLR signaling) may determine NF-κB activity and in turn immunophentoypes in *BRCA1/2* mutation-associated breast cancers. HRD-low cancers also exhibited heightened TGFβ signaling, which is known to promote trans-differentiation of fibroblasts to myofibroblasts, a prominent feature of the HRD-low tumor microenvironment in our investigation (27). Myofibroblasts have previously been associated with sites of inflammation and their depletion has been associated with loss of T-cell effector cells, as we observed (37, 38). Further, an NF-κB positive feedback loop has been shown to maintain activated myofibroblasts in breast tumors through IL6 (39), a pathway which was elevated in HRD low tumors (Supplementary Table S5). Collectively, these data underscore that the inflammation and heightened immune infiltrates observed in HRD-low tumors may be driven by NF-κB, which may promote the presence of stromal myofibroblasts potentially via TGFβ and IL6 signaling.

Our study also highlights the relationship between partial or complete loss of *BRCA1/2* function and immunogenicity in patients with germline *BRCA1/2* mutations. Loss of the non-mutated wild-type allele in breast tumors associated with *BRCA1* or *BRCA2* germline mutations has been commonly reported (40). We have found that absence of *BRCA* locus-specific LOH is more frequent than previously thought, particularly in association with *BRCA2* germline mutations, and that patients with absence of allele-specific LOH in their ovarian cancers have significantly poorer survival when treated with adjuvant platinum therapy and thus may drive intrinsic resistance to this therapy (2). In the current study, we found that breast cancers associated with *BRCA1/2* germline mutations without allele-specific LOH were characterized by a higher cytotoxic $CD8^+$ T-cell infiltrate, elevated markers of cytolytic activity, and increased macrophage membrane PDL1. Moreover, tumors with subclonal somatic mutations in *BRCA1/2* also were more immunogenic than those with clonal somatic mutations. These associations were particularly pronounced in *BRCA1*-deficient cancers when analyzed separately, with generally similar trends observed in *BRCA2*-deficient cancers, suggesting that breast cancers without allele-specific LOH of the germline *BRCA1/2* mutation or demonstrating subclonality of somatic *BRCA1/2* mutations may be more intrinsically responsive to immune checkpoint blockade. Although our findings have important implications for the treatment of breast cancers with *BRCA1* and *BRCA2* alterations, whether patients with low HRD may preferentially respond to immune checkpoint blockade will require direct evaluation in the clinic.

Importantly, hormone receptor expression, previously found to independently influence immunogenicity (6), further stratified tumor immune properties. HRD-low TNBC tumors were the most immunogenic subset characterized by high PD1–PDL1 and TCR signaling, whereas HRD-high receptor-positive tumors were the least immunogenic.

Overall, our study addresses a pressing clinical need to understand the potential causes of heterogeneity in response to immune

checkpoint blockade in breast cancer patients with high-penetrance germline *BRCA1/2* mutations or with somatic alterations in *BRCA1/2*. Our data are consistent with prior reports that *BRCA1/2* mutation-associated tumors are generally more immunogenic than *BRCA1/2* wild type tumors (4–7), and we build on this work by accounting for the wide range in immunogenicity observed in *BRCA1/2* tumors (4) through molecular stratification, which can offer key therapeutic insights. Our study further demonstrates that clinically available molecular genetic testing, namely assessment of tumor HRD, *BRCA1/2* allele-specific LOH, and somatic *BRCA1/2* clonality, coupled with hormone receptor status can be used to stratify breast cancer immunogenicity. As *BRCA1* and *BRCA2* mutations are associated with many other cancer types including ovarian and aggressive prostate cancer, our findings may have applicability beyond breast cancer. Although our study is one of the largest *BRCA1/2* breast tumor analyses to date, a larger sample size would be invaluable to further understand differences in *BRCA1* versus *BRCA2* tumor immunity. Although our study did not specifically address cancers emerging from germline non-*BRCA1/2* HR germline mutations, the evidence to date suggest that such tumors are quite diverse in that some are similar to *BRCA1/2* mutation-associated tumors and display "BRCAness" (e.g., PALB2) whereas others are not BRCA-like (e.g. *CHEK2*, *ATM*; refs. 41, 42). Breast cancers associated with each gene would have to be profiled in equivalent numbers to our *BRCA1/2* mutation-associated cancers, which is outside the scope of the current study.

In sum, the results of our study give novel insights into the relationship between HRD and immunogenicity in breast cancers associated with *BRCA1/2* alterations, which can potentially guide treatment strategies utilizing DNA damaging agents and checkpoint blockade alone or in combination.

Disclosure of Potential Conflicts of Interest

J.J.D. Morrissette reports receiving speakers bureau honoraria from TriCon and CHI NHS Summit, and is a consultant/advisory board member for Novartis and Loxo. S.M. Domchek reports receiving speakers bureau honoraria from AstraZeneca, Clovis, and Bristol-Myers Squibb. R.H. Vonderheide reports receiving speakers bureau honoraria from Celgene and Janssen, is a consultant/advisory board member for Apexigen, AstraZeneca, Genentech, Lilly, MedImmune, Merck, and Verastem, and reports receiving commercial research grants from Apexigen, Fibrogen, Inovio, Janssen, and Lilly. No potential conflicts of interest were disclosed by the other authors.

Disclaimer

The content is solely the responsibility of the authors and does not necessarily represent the official views of the National Institutes of Health.

Authors' Contributions

Conception and design: A.A. Kraya, K.N. Maxwell, M. Feldman, S.M. Domchek, R.H. Vonderheide, K.L. Nathanson

Development of methodology: K.N. Maxwell, A.J. Rech, A. Nayak, R.H. Vonderheide

Acquisition of data (provided animals, acquired and managed patients, provided facilities, etc.): A.A. Kraya, K.N. Maxwell, A. Barrett, J.J.D. Morrissette, M. Feldman, A. Nayak, S.M. Domchek, K.L. Nathanson

Analysis and interpretation of data (e.g., statistical analysis, biostatistics, computational analysis): A.A. Kraya, K.N. Maxwell, B. Wubbenhorst, B.M. Wenz, J. Pluta, A.J. Rech, N. Mitra, J.J.D. Morrissette, M. Feldman, A. Nayak, S.M. Domchek, R.H. Vonderheide, K.L. Nathanson

Writing, review, and/or revision of the manuscript: A.A. Kraya, K.N. Maxwell, N. Mitra, J.J.D. Morrissette, M. Feldman, A. Nayak, S.M. Domchek, R.H. Vonderheide, K.L. Nathanson

Administrative, technical, or material support (i.e., reporting or organizing data, constructing databases): L.M. Dorfman, N. Lunceford, A. Nayak, K.L. Nathanson

Study supervision: R.H. Vonderheide, K.L. Nathanson

Acknowledgments

The authors thank the patients that participated in their studies. The authors further thank E. John Wherry, PhD (University of Pennsylvania), for helpful comments on the manuscript. Financial support for this work was provided by the National Institutes of Health (P30 CA016520), Basser Center for BRCA at the University of Pennsylvania (to K.L. Nathanson, S.M. Domchek, and R.H. Vonderheide), Breast Cancer Research Foundation (to K.L. Nathanson, S.M. Domchek, and R.H. Vonderheide), Susan G. Komen Foundation (to S.M. Domchek), Rooney Family Foundation (to K.L. Nathanson and S.M. Domchek), National Institutes of Health (K12-CA076931; to K.N. Maxwell), Konner Family Foundation (to K.N. Maxwell), Parker Institute for Cancer Immunotherapy (to R.H. Vonderheide, A.J. Rech, and K.L. Nathanson), National Center for Advancing Translational Sciences of the National Institutes of Health (TL1TR001880; to A.A. Kraya), and National Human Genome Research Institute of the National Institutes of Health (5T32HG009495-02; to A.A. Kraya).

The costs of publication of this article were defrayed in part by the payment of page charges. This article must therefore be hereby marked *advertisement* in accordance with 18 U.S.C. Section 1734 solely to indicate this fact.

Received February 15, 2018; revised December 8, 2018; accepted March 15, 2019; published first March 26, 2019.

References

1. Robson M, Im SA, Senkus E, Xu B, Domchek SM, Masuda N, et al. Olaparib for metastatic breast cancer in patients with a germline BRCA mutation. N Engl J Med 2017;377:523–33.
2. Maxwell KN, Wubbenhorst B, Wenz BM, De Sloover D, Pluta J, Emery L, et al. BRCA locus-specific loss of heterozygosity in germline BRCA1 and BRCA2 carriers. Nat Commun 2017;8:319.
3. Telli ML, Timms KM, Reid J, Hennessy B, Mills GB, Jensen KC, et al. Homologous recombination deficiency (HRD) score predicts response to platinum-containing neoadjuvant chemotherapy in patients with triple-negative breast cancer. Clin Cancer Res 2016; 22:3764–73.
4. van Verschuer VM, Hooning MJ, van Baare-Georgieva RD, Hollestelle A, Timmermans AM, Koppert LB, et al. Tumor-associated inflammation as a potential prognostic tool in BRCA1/2-associated breast cancer. Hum Pathol 2015;46:182–90.
5. Parkes EE, Walker SM, Taggart LE, McCabe N, Knight LA, Wilkinson R, et al. Activation of STING-dependent innate immune signaling by S-phase-specific DNA damage in breast cancer. J Natl Cancer Inst 2017;109:djw199.
6. Jiang T, Shi W, Wali VB, Pongor LS, Li C, Lau R, et al. Predictors of chemosensitivity in triple negative breast cancer: an integrated genomic analysis. PLoS Med 2016;13:e1002193.
7. Nolan E, Savas P, Policheni AN, Darcy PK, Vaillant F, Mintoff CP, et al. Combined immune checkpoint blockade as a therapeutic strategy for BRCA1-mutated breast cancer. Sci Transl Med 2017;9. pii: eaal4922.
8. Lakhani SR JJ, Sloane JP, Gusterson BA, Anderson TJ, van de Vijver MJ, Farid LM, et al. Multifactorial analysis of differences between sporadic breast cancers and cancers involving BRCA1 and BRCA2 mutations. J Natl Cancer Inst 1198;90:1138–45.
9. Vonderheide RH, Domchek SM, Clark AS. Immunotherapy for breast cancer: what are we missing? Clin Cancer Res 2017;23:2640–6.
10. Nanda R, Chow LQ, Dees EC, Berger R, Gupta S, Geva R, et al. Pembrolizumab in patients with advanced triple-negative breast cancer: phase Ib KEYNOTE-012 Study. J Clin Oncol 2016;34:2460–7.

11. Davoli T, Uno H, Wooten EC, Elledge SJ. Tumor aneuploidy correlates with markers of immune evasion and with reduced response to immunotherapy. Science 2017;355. pii: eaaf8399.
12. Konstantinopoulos PA, Ceccaldi R, Shapiro GI, D'Andrea AD. Homologous recombination deficiency: exploiting the fundamental vulnerability of ovarian cancer. Cancer Discov 2015;5:1137–54.
13. Rooney MS, Shukla SA, Wu CJ, Getz G, Hacohen N. Molecular and genetic properties of tumors associated with local immune cytolytic activity. Cell 2015;160:48–61.
14. Yoshihara K, Shahmoradgoli M, Martinez E, Vegesna R, Kim H, Torres-Garcia W, et al. Inferring tumour purity and stromal and immune cell admixture from expression data. Nat Commun 2013;4:2612.
15. Gerondakis S, Siebenlist U.Roles of the NF-kappaB pathway in lymphocyte development and function. Cold Spring Harb Perspect Biol 2010;2: a000182.
16. Hopewell EL, Zhao W, Fulp WJ, Bronk CC, Lopez AS, Massengill M, et al. Lung tumor NF-kappaB signaling promotes T cell-mediated immune surveillance. J Clin Invest 2013;123:2509–22.
17. Yang CH, Murti A, Pfeffer SR, Basu L, Kim JG, Pfeffer LM. IFNalpha/beta promotes cell survival by activating NF-kappa B. Proc Natl Acad Sci U S A 2000;97:13631–6.
18. Banerjee A, Gerondakis S.Coordinating TLR-activated signaling pathways in cells of the immune system. Immunol Cell Biol 2007;85:420–4.
19. Raafat A, Bargo S, McCurdy D, Callahan R. The ANK repeats of Notch-4/Int3 activate NF-kappaB canonical pathway in the absence of Rbpj and causes mammary tumorigenesis. Sci Rep 2017;7:13690.
20. Freudlsperger C, Bian Y, Contag Wise S, Burnett J, Coupar J, Yang X, et al. TGF-beta and NF-kappaB signal pathway cross-talk is mediated through TAK1 and SMAD7 in a subset of head and neck cancers. Oncogene 2013;32: 1549–59.
21. Devin A, Cook A, Lin Y, Rodriguez Y, Kelliher M, Liu ZG. The distinct roles of TRAF2 and RIP in IKK activation by TNF-R1: TRAF2 recruits IKK to TNF-R1 while RIP mediates IKK activation. Immunity 2000;12:419–29.
22. Droin N, Hendra JB, Ducoroy P, Solary E. Human defensins as cancer biomarkers and antitumour molecules. J Proteomics 2009;72:918–27.
23. Mouw KW, Goldberg MS, Konstantinopoulos PA, D'Andrea AD. DNA damage and repair biomarkers of immunotherapy response. Cancer Discov 2017;7:675–93.
24. Cai X, Chiu YH, Chen ZJ. The cGAS-cGAMP-STING pathway of cytosolic DNA sensing and signaling. Mol Cell 2014;54:289–96.
25. Hegde PS, Karanikas V, Evers S. The where, the when, and the how of immune monitoring for cancer immunotherapies in the era of checkpoint inhibition. Clin Cancer Res 2016;22:1865–74.
26. Xia Y, Shen S, Verma IM. NF-kappaB, an active player in human cancers. Cancer Immunol Res 2014;2:823–30.
27. Taylor MA, Lee YH, Schiemann WP. Role of TGF-beta and the tumor microenvironment during mammary tumorigenesis. Gene Expr 2011;15:117–32.
28. Chang JY, Kessler HP.Masson trichrome stain helps differentiate myofibroma from smooth muscle lesions in the head and neck region. J Formos Med Assoc 2008;107:767–73.
29. Balli D, Rech AJ, Stanger BZ, Vonderheide RH. Immune cytolytic activity stratifies molecular subsets of human pancreatic cancer. Clin Cancer Res 2017;23:3129–38.
30. Cristescu R, Mogg R, Ayers M, Albright A, Murphy E, Yearley J, et al. Pan-tumor genomic biomarkers for PD-1 checkpoint blockade-based immunotherapy. Science 2018;362. pii: eaar3593.
31. Li J, Byrne KT, Yan F, Yamazoe T, Chen Z, Baslan T, et al. Tumor cell-intrinsic factors underlie heterogeneity of immune cell infiltration and response to immunotherapy. Immunity 2018;49:178–93.e7.
32. Jerby-Arnon L, Shah P, Cuoco MS, Rodman C, Su MJ, Melms JC, et al. A cancer cell program promotes T cell exclusion and resistance to checkpoint blockade. Cell 2018;175:984–97.e24.
33. Sau A, Lau R, Cabrita MA, Nolan E, Crooks PA, Visvader JE, et al. Persistent Activation of NF-kappaB in BRCA1-deficient mammary progenitors drives aberrant proliferation and accumulation of DNA damage. Cell Stem Cell 2016;19:52–65.
34. Benezra M, Chevallier N, Morrison DJ, MacLachlan TK, El-Deiry WS, Licht JD. BRCA1 augments transcription by the NF-kappaB transcription factor by binding to the Rel domain of the p65/RelA subunit. J Biol Chem 2003; 278:26333–41.
35. Habraken Y, Piette J.NF-kappaB activation by double-strand breaks. Biochem Pharmacol 2006;72:1132–41.
36. Volcic M, Karl S, Baumann B, Salles D, Daniel P, Fulda S, et al. NF-kappaB regulates DNA double-strand break repair in conjunction with BRCA1-CtIP complexes. Nucleic Acids Res 2012;40:181–95.
37. Oguejiofor K, Hall J, Slater C, Betts G, Hall G, Slevin N, et al. Stromal infiltration of CD8 T cells is associated with improved clinical outcome in HPV-positive oropharyngeal squamous carcinoma. Br J Cancer 2015;113: 886–93.
38. Ozdemir BC, Pentcheva-Hoang T, Carstens JL, Zheng X, Wu CC, Simpson TR, et al. Depletion of carcinoma-associated fibroblasts and fibrosis induces immunosuppression and accelerates pancreas cancer with reduced survival. Cancer Cell 2014;25:719–34.
39. Hendrayani SF, Al-Harbi B, Al-Ansari MM, Silva G, Aboussekhra A. The inflammatory/cancer-related IL-6/STAT3/NF-kappaB positive feedback loop includes AUF1 and maintains the active state of breast myofibroblasts. Oncotarget 2016;7:41974–85.
40. Smith SA, Easton DF, Evans DG, Ponder BA. Allele losses in the region 17q12–21 in familial breast and ovarian cancer involve the wild-type chromosome. Nat Genet 1992;2:128–31.
41. Lord CJ, Ashworth A. BRCAness revisited. Nat Rev Cancer 2016;16: 110–20.
42. Weigelt B, Bi R, Kumar R, Blecua P, Mandelker DL, Geyer FC, et al. The landscape of somatic genetic alterations in breast cancers from ATM germline mutation carriers. J Natl Cancer Inst 2018;110: 1030–4.
43. Spurdle AB, Healey S, Devereau A, Hogervorst FB, Monteiro AN, Nathanson KL, et al. ENIGMA–evidence-based network for the interpretation of germline mutant alleles: an international initiative to evaluate risk and clinical significance associated with sequence variation in BRCA1 and BRCA2 genes. Hum Mutat 2012;33:2–7.
44. Koboldt DC, Zhang Q, Larson DE, Shen D, McLellan MD, Lin L, et al. VarScan 2: somatic mutation and copy number alteration discovery in cancer by exome sequencing. Genome Res 2012;22: 568–76.
45. Favero F, Joshi T, Marquard AM, Birkbak NJ, Krzystanek M, Li Q, et al. Sequenza: allele-specific copy number and mutation profiles from tumor sequencing data. Ann Oncol 2015;26:64–70.
46. Szolek A, Schubert B, Mohr C, Sturm M, Feldhahn M, Kohlbacher O. OptiType: precision HLA typing from next-generation sequencing data. Bioinformatics 2014;30:3310–6.
47. Karosiene E, Lundegaard C, Lund O, Nielsen M. NetMHCcons: a consensus method for the major histocompatibility complex class I predictions. Immunogenetics 2012;64:177–86.
48. Hanzelmann S, Castelo R, Guinney J. GSVA: gene set variation analysis for microarray and RNA-seq data. BMC Bioinformatics 2013;14:7.
49. Subramanian A, Tamayo P, Mootha VK, Mukherjee S, Ebert BL, Gillette MA, et al. Gene set enrichment analysis: a knowledge-based approach for interpreting genome-wide expression profiles. Proc Natl Acad Sci U S A 2005;102:15545–50.
50. Ritchie ME, Phipson B, Wu D, Hu Y, Law CW, Shi W, et al. limma powers differential expression analyses for RNA-sequencing and microarray studies. Nucleic Acids Res 2015;43:e47.